

Design of Gain-Clamped Doped-Fiber Amplifiers for Optimal Dynamic Performance

Alberto Bononi and Lorenzo Barbieri

Università di Parma, Dipartimento di Ingegneria dell'Informazione, Parma, I-43100, Italy.

Abstract— This paper provides design guidelines for gain-clamped doped-fiber amplifiers in a wavelength division multiplexed networking environment. A simple dynamic model of the doped fiber amplifier allows us to derive explicit expressions for the small-signal response, which help identify and optimize the most critical parameters, pump power and laser wavelength, for best dynamic performance. The pump power should be chosen 1-2 dBs above its required open-loop value, with all channels present, for the required signal gain. The laser wavelength should be placed either close to the unity-gain region of the clamped gain profile, or at its peak.

I. INTRODUCTION

Doped-fiber amplifiers (DFAs) for wavelength division multiplexed (WDM) systems have a non-flat gain-versus-wavelength profile, which greatly varies because of saturation when the input power levels are large. In the design of optically amplified links for WDM applications, in which the number and the power level of the input channels may vary randomly in time as in a networking scenario, it is thus essential to stabilize the amplifier gain profile.

One stabilization technique, known as gain clamping, uses an all-optical feedback lasing signal sustained by the amplifier itself, which clamps the average inversion and thus the gain to the desired level [1]. The feedback is either obtained by forming a feedback fiber loop, effectively implementing a fiber ring laser (loop configuration), or by placing fiber gratings, acting as mirrors only at the laser wavelength, at the active fiber ends (straight-line configuration).

While most design works on gain-clamping deal with the steady-state analysis, a great deal of studies on the transient gain dynamics has recently appeared in the context of all-optical networks [2]–[5].

This paper addresses the design of gain-clamped doped-fiber amplifiers for best dynamic performance, utilizing the simplified dynamic model of the open-loop amplifier introduced in [6]. System theory techniques are used to find small signal transfer functions leading to simple selection criteria for pump power, laser wavelength and loop loss for optimal dynamic performance.

The paper is organized as follows. Section II. introduces the dynamic nonlinear model of the gain-clamped amplifier in loop configuration. Section III. deals with its steady-state analysis. Section IV. introduces the design criteria for optimal dynamic performance, and Section V. derives its linearized model, providing a clear picture of the dynamics inside the gain-clamped DFA, and providing explicit expressions and selection criteria of the key dynamic parameters. Section VI. summarizes the main findings.

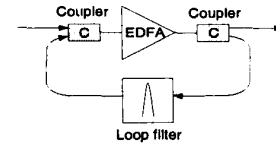


Fig. 1. Gain-clamped amplifier scheme in loop configuration.

II. MODEL

The gain-clamped amplifier under study is shown in Fig. 1. It is composed of a single-section DFA, with a piece of standard fiber feeding part of the output to the DFA input.

The positive optical feedback in the figure causes instability, and if the DFA gain is initially larger than the loop loss, the system starts oscillating at the wavelength selected by the narrowband loop filter centered at wavelength λ_l .

In the assumption of a two-level system for the dopant ions and an homogeneously broadened gain spectrum, and neglecting ASE, the DFA can be modeled as a nonlinear dynamic system with a single state variable, namely its total number of excited ions r , called the *reservoir* [6]. If r_{max} is the total number of ions in the DFA, the normalized reservoir $x \triangleq r/r_{max}$ represents the average fraction of excited ions in the DFA, known as *average inversion*. The update equation for the reservoir is [6]:

$$\dot{r}(t) = \sum_{j \in \{S, p, l\}} Q_j(t) \{1 - G_j(r(t))\} - \frac{r(t)}{\tau} \quad (1)$$

where: τ is the fluorescence lifetime; Q_j , $j \in \mathcal{S} \triangleq \{1, \dots, N\}$ are the input WDM signal fluxes [photons/sec] at wavelengths λ_j , Q_p the input pump flux, Q_l the input laser flux; $G_j(r) = e^{B_j r - A_j}$ is the gain at wavelength λ_j , where B_j and A_j are non-dimensional wavelength dependent coefficients [6].

We then account for the optical feedback by writing the laser input flux as a delayed and attenuated version of the output flux:

$$Q_l(t) = \alpha \{Q_l(t - \tau_l) G_l(r(t - \tau_l))\} \quad (2)$$

being τ_l the loop propagation delay and $0 \leq \alpha \leq 1$ the loop attenuation, both at laser wavelength λ_l .

Equations (1)–(2) form the dynamic model of the gain-clamped amplifier.

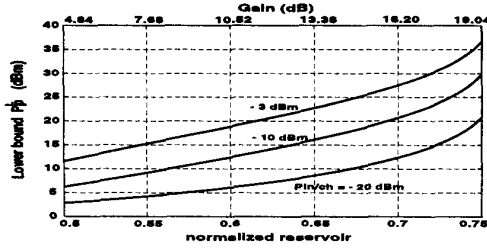


Fig. 2. Lower bound on pump power P_p^L versus average inversion x , with input power per channel as a parameter.

III. STEADY-STATE ANALYSIS

The steady-state is obtained by letting $\dot{r}(t) = 0$ in (1) and $Q_i(t) = Q_i(t - \tau)$ in (2). As a result we get:

$$G_i^{ss} = 1/\alpha \quad (3a)$$

$$Q_i^{ss} = \frac{\sum_{j \in \{S,p\}} Q_j [1 - G_j^{ss}] - \frac{r_{ss}}{\tau}}{1/\alpha - 1}. \quad (3b)$$

where G_j^{ss} is shorthand for $G_j(r_{ss})$. From (3a) we get an explicit expression for the steady state reservoir

$$r_{ss} = \frac{\ln 1/\alpha + A_l}{B_l}. \quad (4)$$

In order to get physically acceptable solutions, the laser flux must be non-negative, so that from (3b) we get:

$$Q_p [1 - G_p^{ss}] \geq \sum_{j \in S} Q_j [G_j^{ss} - 1] + \frac{r_{ss}}{\tau}. \quad (5)$$

which we interpret either as a lower bound on pump flux or as an upper bound on input fluxes. Given the input fluxes $\{Q_j\}$ and the desired reservoir r_{SS} , (5) with the equality sign gives the lower bound on pump Q_p^L , i.e., the pump flux needed in an open-loop (non-clamped) DFA to reach the desired inversion. Using a pump flux $Q_p > Q_p^L$, the net laser flux in (3b) can be rewritten as

$$Q_i^{ss}(1/\alpha - 1) = (Q_p - Q_p^L)(1 - G_p^{ss}). \quad (6)$$

which is independent of laser wavelength.

Let's now consider a numerical example, to which we will often refer. The erbium DFA (EDFA) parameters used are those in [6]. The WDM system is composed of 8 channels with equal input power per channel $P_{in/ch}$ at frequencies chosen according to the ITU-T standard between 192.8 THz (1554.9 nm) and 193.5 THz (1549.3 nm), with 100 GHz (0.8 nm) spacing.

Fig. 2 shows the lower bound on pump power $P_p^L \triangleq h\nu_p Q_p^L$ versus normalized steady-state reservoir, with input power per channel $P_{in/ch}$ as a parameter when all 8 WDM channels are present. Such a minimum pump is the one needed by the open-loop amplifier to guarantee the required gain level and profile with all channels present, and thus to ensure the existence of the laser oscillation in all other possible static configurations of the WDM system.

The reservoir fixes the gain profile and level, which in the middle of the WDM comb has the dB values indicated in the upper "Gain" axis. We observe that for a typical inter-amplifier loss of 10–15 dB the pump lower bound is below 10 dB for signal levels of -20 dBm/ch, below 16 dB for -10 dBm/ch, and as high as 23 dB for a typical value for all-optical networks such as -3 dBm/ch. This means that a very large pump value is already required for open-loop EDFAs to guarantee the required gain and profile.

IV. DESIGN FOR OPTIMAL DYNAMIC PERFORMANCE

In the design of the gain-clamped amplifier we have specifications on the number of WDM signals, input signal power per channel $P_{in/ch}$, and signal gain. Considering that the major cost is due to the large pump power in the DFA, our target is to stabilize a given gain profile, for given input channels and required gain level, by *minimizing* the required pump power.

Since a one-to-one relation exists between gain profile and reservoir value, system specifications fix the required value for r_{ss} at steady state. Given r_{ss} , laser wavelength λ_l and loop loss are related by (4). We have one degree of freedom in the choice between laser loss and wavelength. Another degree is available with the selection of the pump power, for which a lower bound to ensure the existence of the laser oscillation with all channels present was obtained in the previous section.

Some extra pump power above the lower bound is needed to ensure the existence of the laser flux even when all channels are active, in order to satisfy specifications on the maximum overshoot on surviving channels during add/drop operations.

Consider our clamped DFA with average inversion $x = 0.6$ and loop delay $\tau = 0.18 \mu s$ corresponding to 40 m of fiber propagation. Starting with all 8 channels active, we repeated the abrupt drop of 7 channels with various values of the input power per channel, signal gain, laser wavelength and pump power, and recorded the maximum power excursion from steady-state (or overshoot) on the surviving channel. The results are summarized in the dB-overshoot contour plots of Fig. 3. We see for instance that the laser wavelength $\lambda_l = 1530$ nm gives much lower excursions than $\lambda_l = 1570$ nm, and that with at least 1.5 dB extra pump with respect to the lower bound and $\lambda_l = 1530$ nm the maximum power excursion can be kept below 0.2 dB (0.65 dB) for input power per channel $P_{in/ch} = -10$ dBm ($P_{in/ch} = -3$ dBm), for signal gains up to 18 dB.

To get indications on which values to use for the key system parameters determining the dynamic response of the clamped amplifier, we now perform a small-signal analysis, leading to simple approximations of the dynamic response.

V. SMALL-SIGNAL ANALYSIS

The nonlinear system described by (1) and (2) has two state variables, namely the reservoir r and the laser input flux Q_l , which reach steady state under continuous wave (CW) signals. In this section we slightly perturb the state equilibrium point to obtain explicit expressions of the system response to any signal/pump perturbation which causes a small perturbation of the state. Since the clamped DFA is normally saturated by the laser flux [5], neglecting ASE in the model is not a limitation.

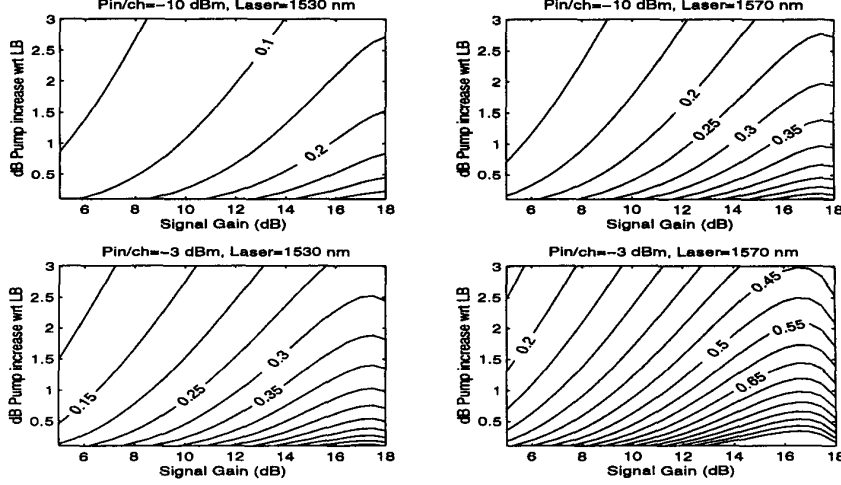


Fig. 3. Contour plots of maximum dB-excursion on surviving channel for a 7 out of 8 channel drop. Y-axis: Q_p/Q_p^L (dB); X-axis: surviving signal gain (dB). Roundtrip delay $\tau_l = 0.18 \mu s$. Contour levels spaced by 0.05 dB.

A. Reservoir Filter

Let the perturbed reservoir be $r(t) \triangleq r_{ss} + \Delta r(t)$ and the perturbed input fluxes be $Q_j(t) \triangleq Q_j^{ss} + \Delta Q_j(t)$, $j \in \{\mathcal{S}, p, l\}$. Assuming that $\max_{j \in \{\mathcal{S}, p, l\}} \{B_j\} \Delta r(t) \ll 1$, we approximate the gain as $G_j(r(t)) = G_j^{ss} e^{B_j \Delta r(t)} \cong G_j^{ss} [1 + B_j \Delta r(t)]$. Using the above expressions in (1), and neglecting the cross-products $\Delta r \Delta Q_j$, we obtain:

$$\dot{\Delta r}(t) = -\frac{\Delta r(t)}{\tau_o} + \sum_{j \in \mathcal{F}} \Delta Q_j(t) (1 - G_j^{ss}) \quad (7)$$

where \mathcal{F} is the set of input fluxes ($\mathcal{F} = \{\mathcal{S}, p\}$ for the unclamped DFA, and $\mathcal{F} = \{\mathcal{S}, p, l\}$ for the clamped DFA), and

$$\frac{1}{\tau_o} \triangleq \frac{1}{\tau} + \sum_{j \in \mathcal{F}} Q_j^{ss} G_j^{ss} B_j. \quad (8)$$

Taking the Laplace transform of both sides of (7) we get a linear relation between the Laplace transform $\Delta R(s)$ of $\Delta r(t)$ and the transform $\Delta Q_j(s)$ of $\Delta Q_j(t)$:

$$\left(s + \frac{1}{\tau_o}\right) \Delta R(s) = \sum_{j \in \mathcal{F}} (1 - G_j^{ss}) \Delta Q_j(s). \quad (9)$$

Equation (9) can be rewritten as

$$\Delta R(s) = K(s) H_o(s) \quad (10)$$

where $K(s) = \sum_{j \in \mathcal{F}} (1 - G_j^{ss}) \Delta Q_j(s)$, and

$$H_o(s) \triangleq \frac{1}{s + \frac{1}{\tau_o}} \quad (11)$$

is the transfer function of a lowpass filter of 3-dB bandwidth $1/\tau_o$ and DC value τ_o . In the absence of optical feedback, the *open-loop* filter $H_o(j\omega)$ passes the low frequency components of the signal/pump flux variations to the reservoir.

The open-loop 3-dB bandwidth increases with the input fluxes.

When optical feedback is present, $\Delta Q_l(s)$ is a function of $\Delta R(s)$. To find such function, we start from equation (2), with the previous expansion of the gain term, to get the laser input flux variation:

$$\Delta Q_l(t) = \Delta Q_l(t - \tau_l) + Q_l^{ss} B_l \Delta r(t - \tau_l). \quad (12)$$

where again we neglected the cross-product $\Delta r \Delta Q_l$. Taking Laplace transforms, and using a first-order Padé rational approximation for the delay term $e^{-\tau_l s} \simeq \frac{1 - \tau_l s/2}{1 + \tau_l s/2}$ [9] we get:

$$\Delta Q_l(s) = \Delta R(s) \frac{Q_l^{ss} B_l}{\tau_l s} \left(1 - \frac{\tau_l}{2} s\right). \quad (13)$$

Using (13) in (9) and the fact that $G_l^{ss} = 1/\alpha$, we get an expression for $\Delta R(s)$ of the same form as (10), where $H_o(s)$ is replaced by the closed-loop transfer function

$$H_c(s) \triangleq \frac{s}{s^2 + \frac{1}{\tau_c} s + \left(\frac{1}{\alpha} - 1\right) \frac{Q_l^{ss} B_l}{\tau_l}} \quad (14)$$

where

$$\frac{1}{\tau_c} \triangleq \left[\frac{1}{\tau} + \sum_{j \in \{\mathcal{S}, p\}} Q_j^{ss} G_j^{ss} B_j \right] + \left(\frac{1}{\alpha} + 1 \right) \frac{Q_l^{ss} B_l}{2}. \quad (15)$$

The denominator in (14) is a second-order polynomial and can be written as [7][8]: $s^2 + 2\xi\Omega_n s + \Omega_n^2 = (s + s_1)(s + s_2)$, where

$$\Omega_n \triangleq \sqrt{\left(\frac{1}{\alpha} - 1\right) \frac{Q_l^{ss} B_l}{\tau_l}} \quad (16)$$

is the *natural system angular frequency*, $\xi \triangleq \frac{1}{2\tau_c\Omega_n}$ the *damping factor*, and s_1 and s_2 the roots, with $|s_1| = |s_2| = \Omega_n$. The underdamped case $\xi < 1$ gives oscillations in the natural system response and complex conjugate roots $s_{1,2} = -\Gamma \pm j\Omega$, where $\Gamma = \frac{1}{2\tau_c}$ is the *decay rate*

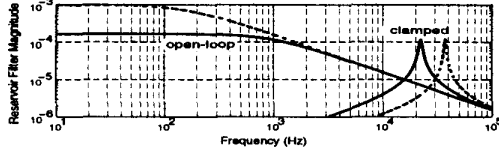


Fig. 4. top: Reservoir filter magnitude, clamped $|H_c(j\omega)|$ and open-loop $|H_o(j\omega)|$. Data: $x = 0.6$, $\tau_l = 0.18 \mu\text{s}$, $\lambda_l = 1530 \text{ nm}$, $P_{in/ch} = -10 \text{ dBm}$, pump power 13.9 dBm for clamped DFA and 12.4 dBm for unclamped DFA. Solid line: 8 channels at steady-state; dashed: 1 channel.

and $\Omega = \Omega_n \sqrt{1 - \xi^2}$ the *relaxation-oscillation angular frequency*. When $\xi < 1$, $H_c(j\omega)$ is a bandpass selective filter, taking peak value τ_c at $\omega = \Omega_n$, and with 3-dB bandwidth $1/\tau_c$.

Fig. 4(top) shows Bode plots of the magnitude of both the open-loop $H_o(j\omega)$ and closed-loop $H_c(j\omega)$ reservoir filters for the same average inversion $x = 0.6$, $P_{in/ch} = -10 \text{ dBm}$, $\lambda_l = 1530 \text{ nm}$ (loop loss 11.85 dB), $\tau_l = 0.18 \mu\text{s}$, closed-loop pump $P_p = 13.9 \text{ dBm}$. To get the same inversion in the open-loop case, a pump of value P_p^L is used. Solid lines correspond to a steady state with all 8 channels present; dashed lines to a steady state with only one channel present. For the same inversion, the top magnitude of the open loop filter is always larger than that of the closed-loop one, since $\tau_o > \tau_c$, although the values are comparable, and so are the 3-dB bandwidths (this is not immediately clear in the log-log Bode plot). Also, both filters roll off as $1/\omega$ for large frequencies, i.e., at a rate of -10 dB/decade. The closed-loop filter does not transmit the low-frequency signal/pump fluctuations to the reservoir; such fluctuations are instead passed by the open-loop filter. This means for example that all the low-frequency relative intensity noise of a cheap pump can effectively be neutralized by clamping. On the other hand, no low-frequency pump overtones can be transmitted to the reservoir and hence impressed on the transiting signals for link monitoring. Moreover, when the steady-state total input power is decreased, as in the figure, the laser flux increases and so does the natural frequency, as per (16). The shift in natural frequency in the example is about 20 kHz. Such strong shift does not allow transmission of pump overtones at the natural frequency, as this is strongly input-signal dependent.

B. Step Response and Choice of Laser Wavelength

If the signals undergo an add/drop discontinuity at time zero: $\Delta Q_j(s) = \frac{\Delta Q_j}{s}$, then by inverse Laplace transforming $\Delta R(s)$ the explicit reservoir variation when $\xi < 1$ is obtained as:

$$\Delta r(t) = \mathcal{K} \frac{e^{-\Gamma t}}{\Omega} \sin \Omega t \quad (17)$$

where $\mathcal{K} = \sum_{j \in \{s,p\}} (1 - G_j^{ss}) \Delta Q_j$.

This is a damped sinusoid, with decay rate Γ and frequency $\frac{\Omega}{2\pi}$.

The time behavior of $\Delta r(t)$ is important, since the dB-power excursion ϵ on any "surviving" channel s after the step variation depends linearly on it as:

$$\epsilon \triangleq 10 \text{Log}_{10} \left\{ \frac{P_s^{out}(r_{ss} + \Delta r(t))}{P_s^{out}(r_{ss})} \right\} = 4.34 B_s \Delta r(t). \quad (18)$$

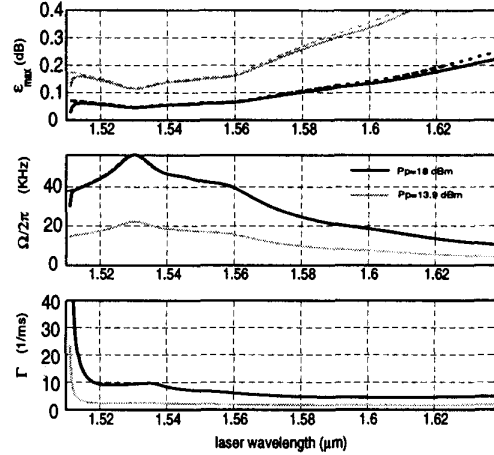


Fig. 5. Maximum dB-power excursion on surviving channel ϵ_{max} , relaxation oscillation frequency Ω and decay rate Γ versus laser wavelength λ_l for a step response to a drop of 7 out of 8 channels. Data: $P_p = 13.9 \text{ dBm}$, $P_{in/ch} = -10 \text{ dBm}$, $x = 0.6$; $\tau_l = 0.18 \mu\text{s}$.

The maximum reservoir variation, or overshoot, is reached in such resonant systems very close to the point where the argument of the sine term is $\pi/2$: $\Delta r_{max} \cong \frac{|\mathcal{K}|}{\Omega} \exp(-\frac{\Gamma}{\Omega} \frac{\pi}{2})$. For strongly resonant systems (i.e. for standard loop loss values larger than a few dBs) the exponential term is close to unity and $\Omega \cong \Omega_n$, so that

$$\Delta r_{max} \cong \frac{|\mathcal{K}|}{\Omega_n} \quad (19)$$

i.e., the reservoir overshoot is roughly inversely proportional to the natural frequency.

Using (6) and the definitions, we rewrite

$$\Omega_n = \sqrt{\frac{B_l}{\tau_l} (Q_p - Q_p^L) (1 - G_p^{ss})}$$

$$\Gamma = \frac{1}{2} \left[\left(\frac{1}{\tau} + \sum_{j \in \{s,p\}} Q_j^{ss} G_j^{ss} B_j \right) + \frac{\frac{1}{\alpha} + 1}{\alpha - 1} \frac{B_l}{2} (Q_p - Q_p^L) (1 - G_p^{ss}) \right] \quad (20)$$

This shows that Ω_n depends on laser wavelength only through the factor B_l , while Γ through the factor $F \triangleq B_l \frac{1/\alpha + 1}{\alpha - 1}$. F should be large for fast oscillation decay. Maximizing B_l maximizes the laser gain variation induced by a given reservoir variation while minimizing the loss maximizes the input laser flux in photons/s as per (3b): in both ways the laser reaction to the add/drop, coming from a decrease/increase of the ions consumed in the reservoir, is improved in speed.

Fig. 5 shows the dependence of the overshoot ϵ_{max} , Ω and Γ on λ_l for a pump of 18 dBm (black) and 13.9 dBm (grey). From the figures and from (20) we see that increasing the pump increases Ω (more oscillations), increases Γ (faster decay), and consequently decreases ϵ (less overshoot). On the graph of Ω (Cfr. [5], Fig. 4) we have superposed the graph of Ω_n in dashed line and the two curves almost exactly overlap on most of the laser range shown, except when λ_l is close

to 1511 nm, where the roots tend to merge and the system loses its high resonance. The dashed lines on the graph of ϵ_{max} represent (18) with approximation (19), and we see that ϵ_{max} is in practice inversely proportional to Ω_n , and reaches its minimum where Ω_n has its maximum, i.e., where B_i is maximum. This implies that at high resonance the most effective laser wavelength to minimize ϵ_{max} for a given pump is the wavelength maximizing B_i , typically around 1530 nm. We also note from (20) that Γ tends to infinity when α tends to one, i.e. close to the critical damping and away from strong resonance. Thus another interesting option for the laser placement is near 1511 nm where the loop loss is close to 1 and laser flux is largest. Although in the loop configuration such low loss is not feasible, the straight-line configuration with large mirror reflectivity at the laser wavelength can get close to that.

It has been pointed out in [10] that the best noise figure is obtained for lowest input laser flux, giving maximum inversion at the input. This corresponds to largest laser loss, and thus 1530 nm is a good choice for both noise figure and dynamic response. However, the principal noise figure degradation in a clamped DFA comes from the WDM signal loss at the input coupler, which should therefore be minimum. According to where the laser is placed, either we can live with a large loop loss and use for example a cheap input 90/10 coupler, or we must use a laser well out of band, so that a wavelength multiplexer can be used, which introduces minimum input signal loss, without too much increase in the laser loop loss. Also, note that a gain-clamped amplifier can only degrade the noise figure with respect to its open-loop counterpart, since without clamping the inversion is always larger when not all WDM channels are present (the laser consumes the extra inversion in the absence of some of the WDM channels).

Finally, a key factor for the choice of laser wavelength is spectral hole burning due to inhomogeneous broadening [5], an effect which is not captured by our model. In essence, the laser wavelength should not be too far from the signals to avoid steady state gain offsets from the desired level. In this regard, 1530 nm is better than 1511 nm, although it is still very far from the signals, usually located in the 1540-1550 nm band.

VI. SUMMARY AND CONCLUSIONS

Starting from a simple state-space model of the DFA, we have provided a detailed analysis of the dynamic behavior of gain-clamped DFAs in a WDM networking environment.

We have provided criteria for the optimal selection of pump power, laser wavelength and laser cavity loss for the design of a gain-clamped DFA with specifications on the number of WDM signals, input signal power per channel, and signal gain. A lower bound on the necessary pump power is given in Fig. 2, and the amount of extra pump needed to satisfy specifications on the maximum overshoot on surviving channels during add/drop operations is given in the contour plots in Fig. 3. From such plots we conclude that the pump power should be chosen 1-2 dBs above its required minimum value. For example, consider a gain-clamped DFA with 8 WDM channels, -3 dBm input signal power per channel, and 12 dB required signal gain. From the graphs we find that a pump power of $20+1.5=21.5$ dBm and a laser placed at 1530 nm ensure a worst-case overshoot

less than 0.25 dB. The required pump value could be obtained using two or more lower power pumps.

While the above plots were derived from the nonlinear model, a linearized analysis lead to simple filters giving the reservoir frequency response to input signal/pump flux perturbations. From these we learned that:

1) in open loop DFA only the low-frequency signal/pump fluctuations are passed to the reservoir and hence to the gain; in clamped DFAs only the fluctuations in a narrow frequency range around the natural system frequency (of the order of some tens of kHz) are passed to the reservoir (Cfr Fig. 4);

2) gain-clamped amplifiers can tolerate pump diodes with large low-frequency relative intensity noise (Cfr Fig. 4);

3) no low-frequency overtones can be impressed on the channels by modulating the pump; overtones at the natural frequency cannot be used, as this is strongly input-power dependent (Cfr Fig. 4);

4) the laser wavelength giving minimum overshoot for loss values larger than a few dBs (hence practical for the loop configuration) is the one maximizing the gain slope B_j , and is usually close to 1530 nm (Cfr Fig. 5);

5) the laser wavelength giving maximum relaxation oscillation damping is the one giving a laser cavity loss very close to 1 (hence interesting for the straight-line configuration), thus having an extremely large laser flux inside the cavity. Such wavelength is close to 1511 nm (Cfr Fig. 5);

The most serious limitation of the model is its assumption of homogeneous broadening. Placing the laser wavelength too far from the signals may cause offsets in the planned steady-state gain due to spectral hole burning, so that our conclusions on the optimal placement of laser wavelength must be weighed against such inhomogeneous effects [5].

Acknowledgments

This work was supported partly by the EU under INCO-DC project No. 950959 "DAWRON", and partly by a grant from CSELT.

REFERENCES

- [1] M. Zirngibl, "Gain control in erbium-doped fiber amplifiers by an all-optical feedback loop," *IEE Electron. Lett.*, vol. 27, pp. 560-561, 1991.
- [2] R. Lebreff, B. Landousies, T. Georges, and E. Delevaque, "Study of power transients in EDFA with gain stabilisation by a laser effect," *IEE Electron. Lett.*, vol. 33, pp. 191-193, Jan. 1997.
- [3] D. H. Richards, M. A. Ali, and J. L. Jackel, "A theoretical investigation of dynamic automatic gain control in multichannel EDFA's and EDFA cascades," *IEEE J. Sel. Areas Quantum Electron.*, vol. 3, pp. 1027-1036, Aug. 1997.
- [4] G. Luo, J. L. Zyskind, Y. Sun, A. K. Srivastava, J. W. Sulhoff, C. Wolf, and M. A. Ali, "Performance degradation of all-optical gain-clamped EDFAs due to relaxation oscillations and spectral hole burning in amplified WDM networks," *IEEE Photon. Technol. Lett.*, vol. 9, pp. 1346-1348, Oct. 1997.
- [5] G. Luo, J. L. Zyskind, J. A. Nagel, and M. A. Ali, "Experimental and theoretical analysis of relaxation-oscillations and spectral hole burning effects in all-optical gain-clamped EDFA's for WDM networks," *IEEE J. Lightwave Technol.*, vol. 16, pp. 527-533, Apr. 1998.
- [6] A. Bononi, L. A. Rusch, "Doped fiber amplifier dynamics: a system perspective", *IEEE J. Lightwave Technol.*, vol. 16, pp. 945-956, May 1998.
- [7] J. Millman, *Microelectronics*, McGraw-Hill, 1979, Ch. 14.
- [8] A. R. Hambley, *Electronics*, MacMillan, 1994, Ch. 8.
- [9] G. F. Franklin, J. D. Powell, and A. Emami-Naeini, *Feedback control of dynamic systems*, Addison Wesley, 1991.
- [10] M. Cai, X. Liu, J. Cui, P. Tang, and J. Peng, "Study on noise characteristic of gain-clamped erbium-doped fiber-ring lasing amplifier," *IEEE Photon. Technol. Lett.*, vol. 9, pp. 1093-1095, Aug. 1997.